PORT SAID ENGINEERING RESEARCH JOURNAL

Faculty of Engineering - Port Said University
Volume (28) No. 4 pp: 53:62

Effects of surface voids on free convection via concentrated double-pipe

Salwa M. Mohamed[1,], Reda A. Khalaf-Allah[2], Mohamed T. Tolan[3], Ammar S. Easa[4]*

[1] *Mechanical Department, Faculty of Technology and Education, Suez University, Suez, Egypt, email: Salwa.Ahmed@ind.suezuni.edu.eg.*
[2] *Mechanical Department, Faculty of Technology and Education, Suez University, Suez, Egypt, email: Reda.Khalafalla@suezuniv.edu.eg.*
[3] *Mechanical Department, Faculty of Technology and Education, Suez University, Suez, Egypt, email: mohamed.tolan@suezuni.edu.eg.*
[4] *Mechanical Department, Faculty of Technology and Education, Suez University, Suez, Egypt, email: Ammar.saad60@suezuniv.edu.eg.*
** Salwa M. Mohamed,* *DOI: 10.21608/PSERJ.2024.301659.1350*

Received 5-7-2024
Revised 3-9-2024
Accepted 8-9-2024

ABSTRACT

Crucial industrial applications that rely on convection over circular concentric gaps between cylinders include solar collectors, heat exchangers, and electronic cooling. In the proposed work, an in-depth laboratory analysis focuses on the impact of cavities on the inner pipe exterior surface on heat transfer via free convection in an encloser's concentric annulus. Twin sets of aluminium cylinders were analyzed; each set had the same length. Two round cylinders, one inside the other, make up each one. An electrical heater is wired into the inner cylinder of the inner set to keep the heat flowing continuously. Results showed that for surface cavities of 0.5, 1.0, 1.5, 2.0, 2.5, 3.0, 3.5, and 4.0 mm deep, the Nusselt number increases by approximately 151%, 201%, 236%, 289%, 325%, 365%, 391%, and 420%, respectively. For a moderate Rayleigh number, the Nusselt number increases by roughly 190%, 276%, 312%, 361%, and 420% for different cavity bores (2.0, 3.0, 4.0, 5.0, and 6.0 mm).

Keywords: Cylindrical cavities, Free convection, Concentric gap, Depth of cavities.

1. INTRODUCTION

Many industrial uses rely heavily on natural convection heat transfer (NCHT), which results from buoyancy in the annular spaces between cylinders, including cooling electrical elements, solar collectors, and thermal exchangers. Fluid motion is picked over natural convection when system reliability, noise, and low power consumption are desired. However, considerable constraints on heat transport are imposed by natural convection due to its fundamentally inferior energy efficiency in comparison to identical or similar forced convection settings. In addition, traditional techniques for improving heat transfer can be applied, including expanded surfaces and turbulators [1–5].

The study of NCHT in a concentrated double pipe with grooves in the inner tube's outer surface has been experimentally investigated [6]. NCHT in an enclosure with a double pipe was studied to determine the influence of annular and longitudinal grooves on the inner tube. According to the findings, a higher Nusselt number is associated with deeper grooves.

The use of nano-fluid to examine NCHT in a concentric annular has been investigated [7]. The influencing factors such as heat source location, average Nusselt number, volume concentration, and Rayleigh number are investigated. The result indicates that the annuli with more heated tubes exhibit enhanced heat transfer capabilities.

Confocal elliptic annulus NCHT has been studied numerically[8]. The effect of hybrid nanoparticles and Rayleigh number on NCHT has been investigated. The results demonstrated that the NCHT rate within the annulus improved with increasing Rayleigh number.

The experimental investigation of NCHT in double pipes was elaborated [9]. The temperature distribution and Nusselt number over the inner tube's surface were analyzed. Since NCHT predominates over the combined heat transfer mechanism, the surface temperature is

higher for low Re numbers than for high Re numbers. The investigation of NCHT in finned annulus was studied [10]. The study of Rayleigh numbers, annulus width, fin arrangements, dimensions, numbers, and geometries has been conducted. NCHT via the annulus improved with increasing Rayleigh number, annulus thickness, width, and number of fins.

The numerical investigation of NCHT in an annular gap of revolving cylinders was examined [11]. Rayleigh numbers, annular gap, and angular speed of cylinders were studied. The outcomes reveal that the rotation of the cylinders significantly impacted the NCHT rate.

The numerical investigation of NCHT in an eccentric annulus with various porous structures has been conducted [12]. Rayleigh number, packed bed structural properties, particle porosity, and diameter have been investigated. The results indicate that these values strongly depend on the sphere's thermal conductivity. Thus, increased porosity or sphere size increases NCHT at a lower conductivity ratio. As porosity or sphere size grows at a medium conductivity ratio, NCHT might increase or decrease. At more excellent thermal conductivity ratios, sphere size or porosity decreases convection heat transfer.

The numerical investigation of NCHT in a concentric annulus with flattened particle hydrodynamics has been studied [13]. Rayleigh number and Prandtl number were explored. The outcome denoted that the NCHT rate increased as the Prandtl and Rayleigh numbers increased.

Free convection from tubes with curved extended surfaces that are arranged vertically was investigated experimentally [14]. The thermal resistance of tubes with curved extended surfaces was compared to conventional tubes, and heat transfer rates under various conditions were measured. 20% less heat resistance was found in tubes with curved extended surfaces.

Furthermore, experimental investigations have been conducted on the influence of opposing eccentricity on natural convection within an enclosed elliptic annular geometry [15]. The cylinders with elliptical cross-sections exhibit a consistent ratio between their diameters and possess equivalent lateral areas. The findings indicate that the lateral opposition of eccentricity enhances the efficiency of NCHT by approximately 40% compared to the concentrical case.

In addition, Casson fluids' double diffusion natural convection in an asymmetrical cavity with a continuous magnetic field was investigated [16]. The results indicated that while a greater Casson parameter decreased mixing, a higher Rayleigh number enhanced convection and entropy. Elevating the buoyancy ratio enhanced mass and heat transmission, whereas a greater Darcy number increased the efficiency of convection.

Experiments on NCHT via an adjacent annulus with an internal elliptic tube have been conducted [17]. The inner elliptical cylinder's orientation was blunt, and its radius ratio was 2. The numerical findings indicate that the heat flux, the tilt angle, and the position of the internal tube of the elliptical cylinder all have a major effect on the streamlined actual behaviour in the annular gap.

NCHT has been studied in turbulent and laminar areas over perpendicular pipes with annulated fins[18]. In both turbulent and laminar streams, the results established a correlation of Nusselt number for perpendicular pipes equipped with annulate fins. These relations were helpful for a large scope of applications, including those in industry and academia.

NCHT via a set of concentrical tubes has also been studied, with particular attention paid to the effect of the angle of attack of the inner cylinder [19]. The cross-section of the inner cylinder was elliptical, while that of the external tube was smoothed. Convective heat transmission increased with increasing the instance angle of the interior pipe.

NCHT through a circular cylinder has been examined statistically by [20], and the influence of inner cylinder size has been found to vary. Heat transmission decreased as the inner cylinder diameter increased, probably because of reduced flow within the annular space. NCHT was studied by [21] by looking at how an electrically heated cylinder of length interacts with a space of air. A study into eccentric pipes was performed in six distinct phases for a concentric casing. The outcomes imply that the NCHT rate is more significant for eccentric tubes. NCHT has been studied [22] between rotating inner and exterior cylinders with toroidal grooves on the outside. The consequences showed that a critical influence on NCHT improvement was achieved by increasing the revolving speed while reducing the groove's aspect ratio.

Horizontal concentric annuli of varying inner forms have been studied during NCHT [23]. Comparably, the simulation has been divided into four categories: square, elliptical, triangular, and cylindrical, depending on the shape of the internal component. Radiation from the surface, sharp corners, and more air space at the top increase heat transfer. As the temperature of reference rises, the role of surface radiation in total NCHT becomes more critical. The use of the Taguchi investigational model for analyzing and enhancing the performance of heat exchangers with helically grooved shells and tubes was also explored [24]. The external surface of the internal tube and the shell's internal surface were studied to see how helical grooves affected both. The helical grooves' varying heights up to 10 mm were predetermined. The helical grooves improved thermal efficiency by around 49%, while the heat transmission rate rose by 5%.

The impact of the geometry of cavities on heat and pressure flow in cavities yields unique advantages in different applications [25–27]. Based on the earlier review and the author's present comprehension, enhancing the NCHT in a circular annular space is paramount. Consequently, the proposed work objectives are to explore the impact of cylindrical cavities on the

outside surface of an inner pipe within an enclosure concentrical circular annulus, as this phenomenon has not been previously examined.

2. EXPERIMENTAL WORK

NCHT in an enclosed cylindrical circular annulus is studied experimentally by adding cavities on the interior cylinder's external surface. The depth and bore of the cavities are experimentally investigated. Two sets of circular tubes having a thermal conductivity of 237 W/m.K and an emissivity of 0.03 with a radius ratio of 2 and lengths of 250 mm were studied. The cylinders were manufactured from aluminium using a JSEDM wire-cut machine. An electric heater is positioned inside the inner tube to maintain consistent heat flux on the internal surface of the internal pipe. The main dimensions of the investigated cylinders are recorded in a table. 1. Fig.1.a shows the cylindrical cavities distribution on the inner cylinder surface. The cylinder has many cylindrical cavities. The cylindrical cavity is distributed around the cylinder in longitudinal lines equal to 18. Each line has 24 circular cavities with an inline distance of 10 mm. Fig.1.b directs the cases of the experimental study with different cavity diameters.

Table 1. The dimensions of the investigated pipes.

Studied Cases	Item Explanation	Dimensions, mm				Cavities diameter
		Inner radius	Outer radius	Length	Thick	
Pair (A)	Outer pipe	45	50	250	5	-
	Inner pipe	20	25	250	5	2
Pair (B)	Outer pipe	45	50	250	5	-
	Inner pipe	20	25	250	5	3
Pair (C)	Outer pipe	45	50	250	5	-
	Inner pipe	20	25	250	5	4
Pair (D)	Outer pipe	45	50	250	5	-
	Inner pipe	20	25	250	5	5
Pair (E)	Outer pipe	45	50	250	5	-
	Inner pipe	0	5	250	5	6

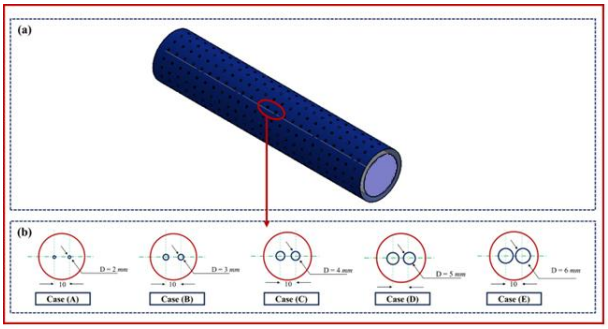

Figure 1: A schematic drawing of the pipe's distribution of the cylindrical cavity.

Each case of cavity diameter is investigated at various cavity depths. The dimensions of the cavity's various depths used in the experiment are shown in Fig. 2. Meanwhile, eight depths are tested for each cavity diameter. Also, Table. 2 lists the experiment codes and their cavities details.

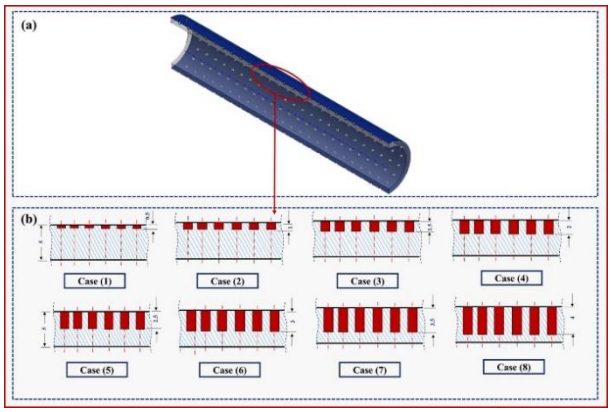

Figure 2: A schematic illustration of the pipe section shows the cavity's various depths.

Table 2. The experiment codes and their cavities details.

Experiment code	Cavities diameter (mm)	Cavities depth (mm)	Experiment code	Cavities diameter (mm)	Cavities depth (mm)
Pair A1	2.0	0.5	Pair C5	4.0	2.5
Pair A2	2.0	1.0	Pair C6	4.0	3.0
Pair A3	2.0	1.5	Pair C7	4.0	3.5
Pair A4	2.0	2.0	Pair C8	4.0	4.0
Pair A5	2.0	2.5	Pair D1	5.0	0.5
Pair A6	2.0	3.0	Pair D2	5.0	1.0
Pair A7	2.0	3.5	Pair D3	5.0	1.5
Pair A8	2.0	4.0	Pair D4	5.0	2.0
Pair B1	3.0	0.5	Pair D5	5.0	2.5
Pair B2	3.0	1.0	Pair D6	5.0	3.0
Pair B3	3.0	1.5	Pair D7	5.0	3.5

Pair B4	**3.0**	**2.0**	**Pair D8**	**5.0**	**4.0**
Pair B5	**3.0**	**2.5**	**Pair E8**	**6.0**	**0.5**
Pair B6	**3.0**	**3.0**	**Pair E8**	**6.0**	**1.0**
Pair B7	**3.0**	**3.5**	**Pair E8**	**6.0**	**1.5**
Pair B8	**3.0**	**4.0**	**Pair E8**	**6.0**	**2.0**
Pair C1	**4.0**	**0.5**	**Pair E8**	**6.0**	**2.5**
Pair C2	**4.0**	**1.0**	**Pair E8**	**6.0**	**3.0**
Pair C3	**4.0**	**1.5**	**Pair E8**	**6.0**	**3.5**
Pair C4	**4.0**	**2.0**	**Pair E8**	**6.0**	**4.0**

The structure of each test sample contains two concentric cylinders, with the inner tube's outer surface having a cylindrical cavity and a cartridge heater is inserted inside the inner pipe, as displayed in Fig.3.

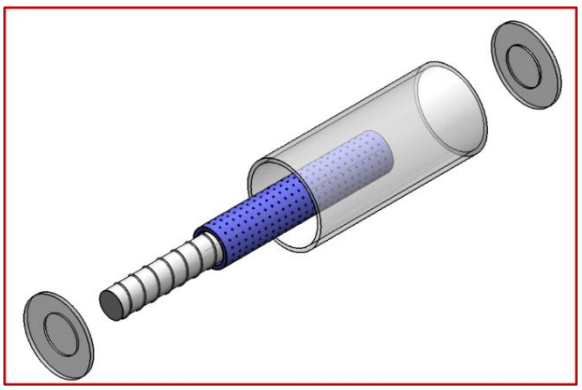

Figure 3: A graphic illustration of the test sample.

Each test sample has eight various depths of cavities. Fig. 4. displays a graph figure of the present test section of the cylindrical cavity. There are 432 cylindrical cavities for each sample. Each model varied in the depth of the cylindrical cavity. Five specimens have various cylindrical cavities with diameters 2, 3, 4, 5, and 6 mm. Every specimen was tested at eight cavities with depths of 0.5, 1.0, 1.5, 2.0, 2.5, 3.0, 3.5, and 4.0 mm.

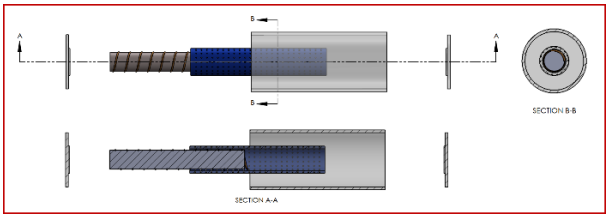

Figure 4: A diagram of the proposed test sample.

2.1 Experimental approach

Fig. 5 (A&B). shows the experimental test approach that involves a pair of concentrical circular pipes, a heating element, a power input system, and a measuring system. The heating element is made of nickel nickel-chrome and installed in the inner circular pipe to generate a variable heat flux for the tested section regularly. Each test sample was oriented horizontally. Both circular annulus ends of the test samples were closed by stuffing thermal Polytetrafluoroethylene (PTFE) to form the enclosure cylindrical annulus space. The thermal PTFE stuffing also fixed both pipes to be concentric. The outside diameter of the annular stuffing is equivalent to the inside bore of the exterior pipe.

In contrast, the inner diameter of the annular stuffing equates to the outer diameter of the inner pipe. Using an isolated frame, the outer pipe is completely affixed inside a glass enclosure, effectively preventing air movement around the specified test segment. An autotransformer regulates the voltage drop across a heater and, therefore, the heat flux. Moreover, the table. 3 shows the measuring device, location, accuracy, and uncertainty.

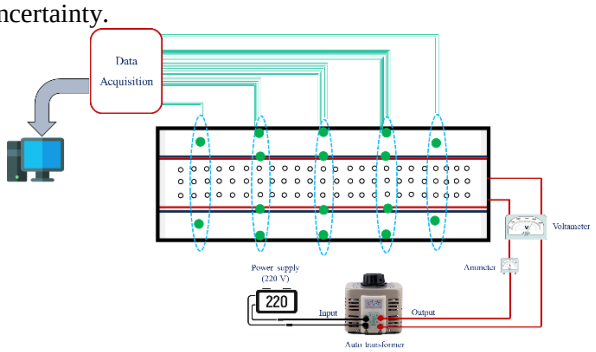

(a)

(b)

Figure 5: (a) a schematic diagram of the experimental approach and (b) the experimental approach.

Table 3. The measuring device, location, accuracy, and uncertainty.

Parameter	Device	Location	Accuracy
Temperature	**Data acquisition**	**In three sections of a pipe**	**± 0.1° C**
Voltage drop	**A MetraHit X-tra multimeter**	**Across the heater**	**±0.05%**
Current	**Ammeter**	**Output of autotransformer**	**± 10 nA**

The temperatures in different locations were determined using 45 K-type thermocouples. Both the outer surface temperatures of the inner tube, as shown in Fig. 6, and the inner surface temperatures of the outer tube, as shown in Fig. 7, were measured using eighteen thermocouples. The thermocouples were spatially

distributed into three separate sections, each containing six thermocouples. The angular distance between each thermocouple was measured at 60°, while the angular displacement between two consecutive sections was 20°.

The air temperature inside the annular space among the pipes was measured using four thermocouples on each side (four thermocouples centred in the middle of the circular annular at each end with an angular distance between each one of 90 degrees). A single thermocouple monitors the ambient temperature inside.

The steady-state condition was confirmed within a time frame of around 3 to 5 hours, depending on the heat flux levels. In order to verify this, the threshold for achieving a steady state condition was established by setting the maximum allowable temporal and spatial changes in temperature measurement to be ±0.1°C over a period of 15 minutes.

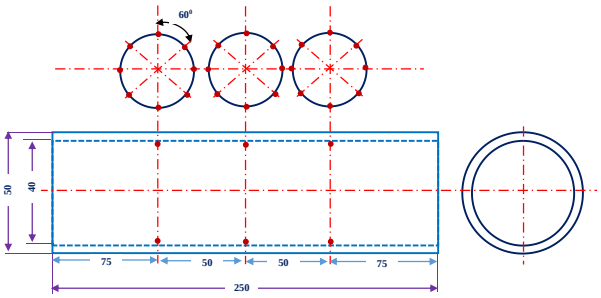

Figure 6: The position of installing thermocouples in the inner pipe.

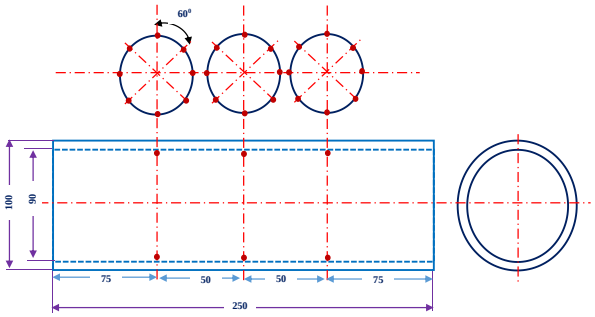

Figure 7: The position of installing thermocouples in the outer pipe.

2.2 Data reduction

The heat transfer process between circular cylindrical annulars via free convection is described as follows. [6,15]:

$$\dot{Q}_{conv} = \dot{Q}_t - \dot{Q}_{rad} - \dot{Q}_{cond} = VI - \dot{Q}_{rad} - \dot{Q}_{cond} = qA_i \quad (1)$$

The radiation heat transfer between inner and outer cylinders is described as follows.

$$\dot{Q}_{rad} = \sigma A_i \varepsilon_i \left(T_{i,a}^4 - T_{air}^4\right) + \left[\frac{\sigma A_i \varepsilon_i \left(T_{i,a}^4 - T_o^4\right)}{\frac{1}{\varepsilon_i} + \frac{1-\varepsilon_o}{\varepsilon_i}}\right] \quad (2)$$

The conduction heat transfer along inner cylinders is described as shown in Fig. 8 as follows[28]

$$\dot{Q}_{cond} = \frac{(T_m - T_e)}{2\left(\frac{L}{k_s A_t}\right)} \quad (3)$$

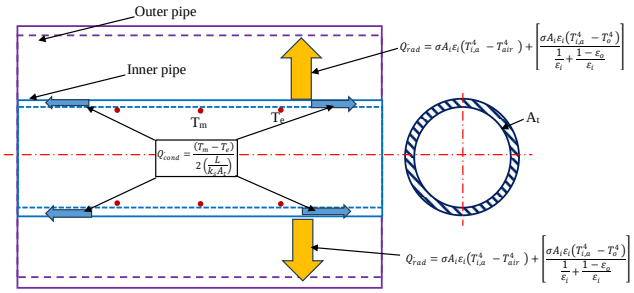

Figure 8: A schematic sketch of different modes of heat transfer in the present work.

The determination of the characteristics of air is conducted at the average temperature, sometimes referred to as the film temperature, which is specified as:

$$T_f = \frac{T_s + T_i}{2} \quad (4)$$

The volumetric expansion coefficient of the air was determined in all experiments (β):

$$\beta = \frac{1}{T} \quad (5)$$

The following equation determines the estimate of the coefficient of convective heat transfer :

$$h = \frac{q''}{\left(T_{i,a} - T_O\right)} \quad (6)$$

The Nusselt and Rayleigh numbers are computed using the following equations., [21]:

$$Nu = \frac{hd_h}{k} \quad (7)$$

$$Gr = \frac{g\beta q {d_h}^4}{k\vartheta^2} \quad (8)$$

$$Ra = Gr \times Pr \quad (9)$$

2.3 Uncertainty analysis:

To assess the degree of uncertainty in a measurement. To approximate the standard uncertainty, use the following equation [29]. Table (4) shows the device's uncertainty, measurement range, and accuracy.

$$U = \frac{\alpha}{\sqrt{3}} \quad (10)$$

Where U is the standard uncertainty and α is the device accuracy.

Table 4. Uncertainty of devices.

Device	Accuracy	Uncertainty
Temperature	**± 0.1° C**	**0.05**
Voltage drop	**±0.05%**	**0.02**
Current	**± 10 nA**	**5.77**

Furthermore, the following equations estimate the uncertainty in every investigative result [6].

$$R=f\,(z1, z2, z3, \ldots\ldots\ldots\ldots zn) \tag{11}$$

$$\Delta R = \sqrt[2]{\left(\frac{\partial U}{\partial z_1}\delta_1\right)^2 + \left(\frac{\partial U}{\partial z_2}\delta_2\right)^2 + \left(\frac{\partial U}{\partial z_3}\delta_3\right)^2 + \cdots + \left(\frac{\partial U}{\partial z_n}\delta_n\right)^2} \tag{12}$$

$$UR = \frac{\Delta R}{R} * 100 \tag{13}$$

While U stands for the degree of uncertainty, R represents the experimental outcome. However, the Nusselt Number uncertainty is about 0.05479, and the Rayleigh Number uncertainty is about 0.02429.

3. RESULTS AND DISCUSSION

Free convection arises due to the vertical movement of fluid resulting from variations in density induced by thermal effects. This work examines the phenomenon of NCHT occurring among twin concentrical circular tubes with similar radius ratios. The results are shown using dimensionless parameters: the Ra and the Nu numbers. The current analysis focuses on the Nu number in the lack of cavities. The data from the plain tube is collected to provide a reference point for comparing the data from the cavities tube. The results focus on the effect of cavities on the internal diameter's external surface.

3.1 Influence of inner pipe with cylindrical cavities on Nusselt number

The study investigated the impact of cylindrical cavities on the external surface of the interior pipe on the rate of NCHT, considering various depths of the cylindrical cavities and Ra numbers. Figure 9 illustrates the relationship between the Ra number and the Nu number in the context of using cavities on the external surface of an inner tube with a bore of 2.0 mm and a depth of 0.5 mm.

The plain internal pipe had the lowest Nu number at different Ra numbers. It has been discovered that the Nusselt number rises when the Rayleigh number increases, which may be attributed to the enhanced heat flow. Furthermore, it has been shown that the addition of cavities on the outer surface of the internal cylinder leads to enhancements in both the surface area and the coefficient of heat transfer due to thermal enlargement. The air close to the inner pipe ascends.

The inner surface of the exterior pipe afterwards facilitates the cooling of the ascending plume. The denser air undergoes a progressive downward movement over the surface of the outer pipe. Consequently, the development of a non-circular vortex occurs, whereby the centres of the more intense vortices undergo an upward shift. In contrast, the centres of the less intense vortices experience a downward movement.

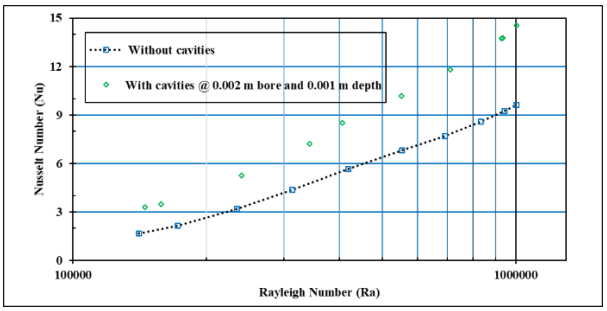

Figure 9: The impact of the Ra NO. on the Nu NO. using cylindrical cavities.

The presence of cavities enhances the level of air circulation at the surface of those cavities. According to the findings shown in Figure 10, it can be seen that for a moderate Rayleigh number, there is a significant relationship between the rise in the depth of the cavities and the corresponding improvement in the Nu number. Specifically, the Nu number experiences an approximate increase of 37.5%, 52.2%, 97%, 111.7%, 136.6%, 142.4%, 157.7%, and 165.1% for cavities depths of 0.5, 1.0, 1.5, 2.0, 2.5, 3.0, 3.5, and 4.0 mm, respectively.

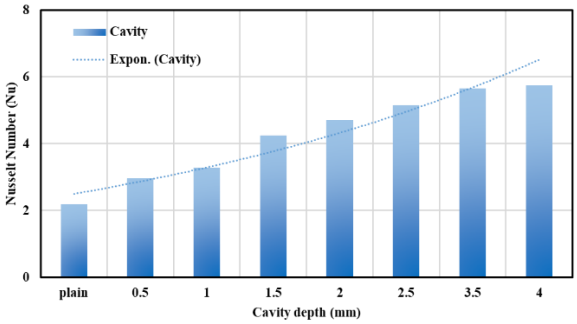

Figure 10: The impact of cavities depth on the Nu NO. at a modest Ra NO.

3.2 The effect of the depth of the cylindrical cavities on heat transfer at various cavities bores

The NCHT rate was estimated for different Ra numbers and depths of cylindrical cavities, considering varied Ra numbers and depths of cylindrical cavities. Figure 11 depicts the impact of the Rayleigh number on various depths of cylindrical cavities with a hollow bore

of 2.0 mm, as determined by the Ra number. The correlation between the Nu number and the Rayleigh number was demonstrated for the plain inner cylinder, as seen from the available data. The Nu number exhibits an upward trend as the Rayleigh number is elevated, owing to the augmented heat transfer.

Moreover, as the depth of the cylindrical cavities increases, there is a corresponding increase in both the surface area and coefficient of heat transmission. Thermal enlargement results from the upward movement of the air located at the outer surface. The cold surface of the outer cylinder effectively lowers the temperature of the ascending plume, resulting in the downward movement of denser air along its surface. Consequently, vortices that are not circular in shape are generated. The middle of practical vortices exhibits an upward movement, while the developments of weaker vortices undergo a downward shift. The presence of cylindrical cavities enhances the flow of air around the surface of those cavities.

Figure 11 illustrates the relationship between the Ra number and the Nu number over several depths of cylindrical cavities with a fixed cavity bore of 2.0 mm. It is viewed that, for a modest Ra number, the depths of the cavities (0.5, 1.0, 1.5, 2.0, 2.5, 3.0, 3.5, and 4.0 mm) result in a rise in the Nu number. by roughly 77.3%, 96%, 113%, 129%, 136%, 153%, 177%, and 190%.

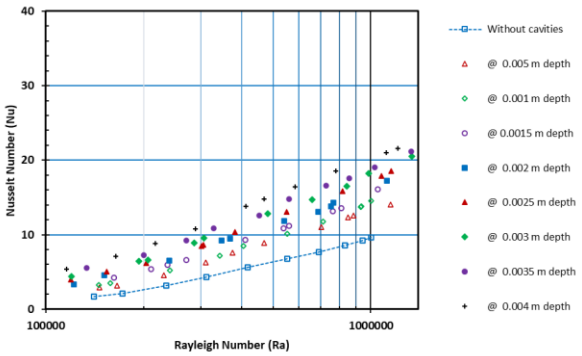

Figure 11: The impact of the Ra No on the Nu No over various depths of cylindrical cavities at a cavity bore of 0.002 m.

Figure 12 depicts the correlation between the Ra No and the Nu No over numerous depths of cylindrical cavities while maintaining a constant cavity bore of 3.0 mm. The data indicates that, for a relatively low Rayleigh number, the Nusselt number experiences a proportional increase as the depths of the cavities (ranging from 0.5 to 4.0 mm) increase. Specifically, the Nusselt number demonstrates an approximate growth of 82%, 99%, 124%, 155%, 170%, 223%, 252%, and 276% for each respective cavity depth.

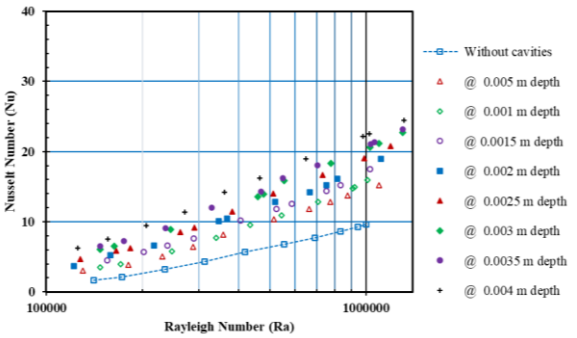

Figure 12: The impact of the Ra No. on the Nu No over various depths of cylindrical cavities at a cavity bore of 0.003 m.

Figure 13 depicts the relationship between the Ra No and the Nu No over varying depths of cylindrical cavities while maintaining a constant cavity bore of 4.0 mm. It has been discovered that, when considering a Rayleigh number of moderate magnitude, the varying depths of the cavities (0.5, 1.0, 1.5, 2.0, 2.5, 3.0, 3.5, and 4.0 mm) lead to an approximate rise in the Nusselt number of 112%, 142%, 168%, 189%, 205%, 251%, 278%, and 312%.

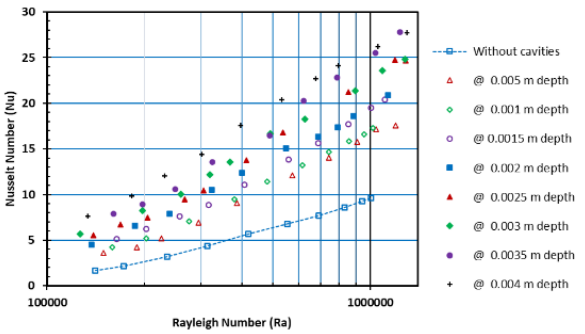

Figure 13: The impact of Ra No on the Nu No over various depths of cylindrical cavities at a cavity bore of 0.004 m.

Cylindrical cavities with a constant bore of 5.0 mm appear in Figure 14 to demonstrate the link between the Ra number and the Nu number at varying depths. For a low Ra number, a rise in Nu number of about 136%, 161%, 196%, 249%, 282%, 305%, 331%, and 361% is observed as a function of cavity depth (0.5, 1.0, 1.5, 2.0, 2.5, 3.0, 3.5, and 4.0 mm).

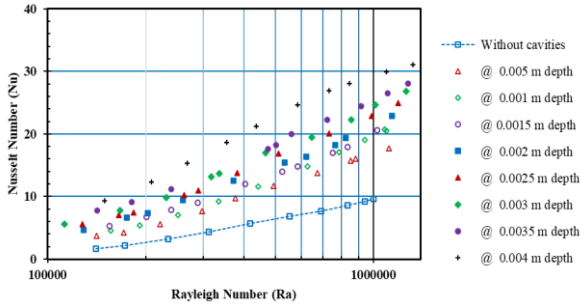

Figure 14: The impact of the Ra No on the Nu No over various depths of cylindrical cavities at a cavity bore of 0.005 m.

Cylindrical cavities with a constant bore diameter of 6.0 mm are shown in Figure 15 to demonstrate the link between the Ra and the Nu numbers at varying depths. For a low Ra number, it is seen that increasing the cavity depth by 151%, 201%, 236%, 289%, 325%, 365%, 391%, and 420% leads to a corresponding improvement in the Nu number.

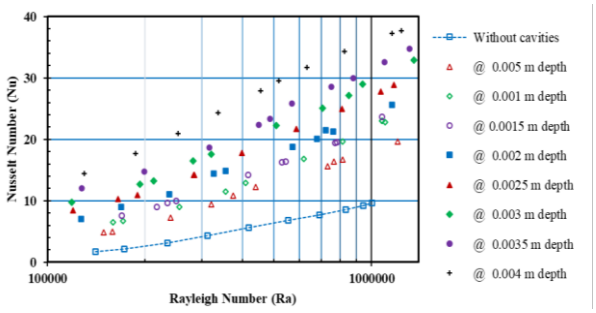

Figure 15: The impact of the Ra No on the Nu No over various depths of cylindrical cavities at a cavity bore of 0.006 m.

3.3 The effect of the bore of the cylindrical cavities on NCHT at the same cavities depth

Furthermore, the surface area of NCHT and the coefficient of heat transfer increase in tandem with the rise in the bore of the cylindrical cavities. When air heats up, it expands and forces the air near the internal surface to rise. Denser air sinks along the outer cylinder's surface because its colder temperature effectively lowers the temperature of the rising plume. As a result, irregularly shaped vortices are produced. A powerful vortex's centre will go higher, whereas a weak one's core will move downward. Having cylindrical voids improves the airflow around their surfaces.

Figure 16 shows the correlation between the Rayleigh and Nusselt numbers for cylindrical cavities of varying bores and a constant depth of 4.0 mm in the cavity. It is seen that the Nusselt number rises by about 190 percent, 276 percent, 312 percent, 361 percent, and 420 percent for a moderate Rayleigh number depending on the cavity bores (2.0, 3.0, 4.0, 5.0, and 6.0 mm).

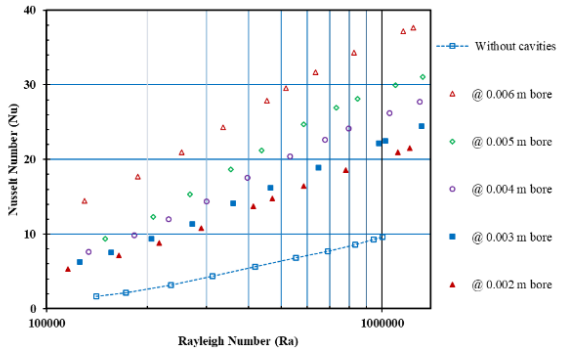

Figure 16: The impact of the Ra No on the Nu No over various cavity bores of cylindrical cavities at cavity depths of 0.004 m.

3.4 Contrast between current and prior work

Figure 17 presents the comparative analysis between our study and other relevant publications. A study of NCHT in an oval-shaped annular enclosure through experimentation [30]. NCHT within the elliptical annulus was studied by [15]. How much heat can be transferred from a long, vertically heated cylinder to a thin, elliptical annular enclosure with a concentric and eccentric air gap has been investigated. [21] .Natural convection was used to analyze heat transfer from a series of horizontally arranged concentric cylinders filled with nano-fluids. [31]. Hybrid nano-fluids have been investigated for their potential to improve natural convection. [32]. As can be seen in Figure 17, the most recent experimental results agree well with the historical data. Figure 17 shows that free convection can be increased by 42% when cavities that are 4.0 mm deep and 6.0 mm in the bore at a high level of Rayleigh number.

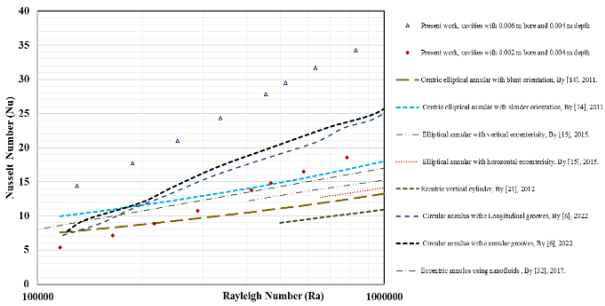

Figure 17: Comparison between present and recent studies.

4. CONCLUSION

The current study examines the effect that cavities on the outer surface of the inner cylinder have on NCHT within a concentrical circular annulus encloser. The research led to the following conclusion:

1- The Nusselt number rises as the depth and bore of surface cavities grow.

2- Nusselt number increased by 151%, 201%, 236%, 289%, 325%, 365%, 391%, and 420% for surface cavities ranging from 0.5 to 4.0 mm deep.

3- The Nusselt number climbs by 190, 276, 312, 361, and 420 percent for a moderate Rayleigh number at a constant depth of 0.04 m depending on cavity bores (2.0, 3.0, 4.0, 5.0, and 6.0 mm)

4- High Rayleigh numbers at 4.0 mm depth and 6.0 mm bore cavities promote free convection by 42%.

5. ABBREVIATIONS

Nomenclature

Signs	Explanation
A	Area, m^2
V	Voltage *(Volt)*
I	Electric current *(Ampere)*
T	Temperature *(K)*
L	Cylinder length *(m)*
Gr	Grashof No.
g	Gravitational acceleration, m/s^2
h	Coeff. of heat transfer, $W/(m^2.K)$
k	Therm. Conductivity, $W/(m.K)$
Nu	Nusselt No.
Pr	Prandtl No.
q	Heat flux, W/m^2
Ra	Rayleigh No.
t	Thickness, m

Greek letters

Signs	Explanation
β	The expansion coefficient, 1/ K
ε	Emissivity
σ	Boltzmann constant, W/m^2K^4

Subscripts

Signs	Explanation
cond	Conduction
conv	Convection
rad	Radiation
a	Average
i	Internal
m	Middle-section
t	Total

6. REFERENCES

[1] L.K. Saha, S.K. Bala, N.C. Roy, Natural convection of dusty nano-fluids within a concentric annulus, The European Physical Journal Plus 2020 135:9 135 (2020) 1–20. https://doi.org/10.1140/EPJP/S13360-020-00759-0.

[2] A. Shadlaghani, M. Farzaneh, M. Shahabadi, M.R. Tavakoli, M.R. Safaei, I. Mazinani, Numerical investigation of serrated fins on natural convection from concentric and eccentric annuli with different cross sections, J Therm Anal Calorim 135 (2019) 1429–1442. https://doi.org/10.1007/S10973-018-7542-Y/FIGURES/12.

[3] S. Husain, M. Adil, M. Arqam, B. Shabani, A review on the thermal performance of natural convection in vertical annulus and its applications, Renewable and Sustainable Energy Reviews 150 (2021) 111463. https://doi.org/10.1016/J.RSER.2021.111463.

[4] M. Kaewbumrung, A. Charoenloedmongkhon, Numerical Simulation of Turbulent Flow in Eccentric Co-Rotating Heat Transfer, Fluids 2022, Vol. 7, Page 131 7 (2022) 131. https://doi.org/10.3390/FLUIDS7040131.

[5] R. Saini, B. Gupta, A. Prasad Shukla, B. Singh, P. Baredar, A. Bisen, CFD analysis of heat transfer enhancement in a concentric tube counter flow heat exchanger using nano-fluids (SiO2/H2O, Al2O3/H2O, CNTs/H2O) and twisted tape turbulators, Mater Today Proc 76 (2023) 418–429. https://doi.org/10.1016/J.MATPR.2022.12.044.

[6] R.A. Khalaf-Allah, E.I. Eid, AEHA Ellithy, A.S. Easa, Experimental Investigation of The Influence of Modifying the Inner Tube Outer Surface on Free Convection in A Concentrated Double Pipe, Https://Doi.Org/10.1080/08916152.2022.2142701 (2022). https://doi.org/10.1080/08916152.2022.2142701.

[7] Y. Ma, M. Jamiatia, A. Aghaei, M. Sepehrirad, A. Dezfulizadeh, M. Afrand, Effect of differentially heated tubes on natural convection heat transfer in a space between two adiabatic horizontal concentric cylinders using nano-fluid, Int J Mech Sci 163 (2019) 105148. https://doi.org/10.1016/J.IJMECSCI.2019.105148.

[8] T. Tayebi, H.F. Öztop, Entropy production during natural convection of hybrid nano-fluid in an annular passage between horizontal confocal elliptic cylinders, Int J Mech Sci 171 (2020) 105378. https://doi.org/10.1016/J.IJMECSCI.2019.105378.

[9] H.A. Mohammed, A. Campo, R. Saidur, Experimental study of forced and free convective heat transfer in the thermal entry region of horizontal concentric annuli, International Communications in Heat and Mass Transfer 37 (2010) 739–747. https://doi.org/10.1016/J.ICHEATMASSTRANSFER.2010.04.007.

[10] S.A. Nada, MA Said, Effects of fins geometries, arrangements, dimensions and numbers on natural convection heat transfer characteristics in finned-horizontal annulus, International Journal of Thermal Sciences 137 (2019) 121–137. https://doi.org/10.1016/J.IJTHERMALSCI.2018.11.026.

[11] DD. Das, B.K. Rana, J.K. Patel, P. Ghose, S.K. Nayak, Combined effect of annular space and rotation on heat transfer from concentric cylinders, Mater Today Proc (2023). https://doi.org/10.1016/J.MATPR.2023.05.397.

[12] G.F. Al-Sumaily, H.M. Hussen, M.T. Chaichan, H.A. Dhahad, M.C. Thompson, Numerical analysis of the effect of porous structure on free convection heat

transfer inside an eccentric annular space, Thermal Science and Engineering Progress 37 (2023) 101579. https://doi.org/10.1016/J.TSEP.2022.101579.
[13] X. Yang, S.C. Kong, Numerical study of natural convection in a horizontal concentric annulus using smoothed particle hydrodynamics, Eng Anal Bound Elem 102 (2019) 11–20. https://doi.org/10.1016/J.ENGANABOUND.2019.02.007.
[14] D. Kim, D.K. Kim, Experimental study of free convection from vertical tubes with curved extended surfaces, International Communications in Heat and Mass Transfer 152 (2024) 107246. https://doi.org/10.1016/J.ICHEATMASSTRANSFER.2024.107246.
[15] E.I. Eid, M. Abdel-Halim, A.S. Easa, Effect of opposed eccentricity on free convective heat transfer through elliptical annulus enclosures in blunt and slender orientations, Heat and Mass Transfer/Waerme-Und Stoffuebertragung 51 (2015) 239–250. https://doi.org/10.1007/s00231-014-1408-z.
[16] M.S. Khan, S. Ahmad, Z. Shah, A. Alshehri, N. Vrinceanu, H. AL Garalleh, Computational study of double diffusive MHD natural convection flow of non-Newtonian fluid between concentric cylinders, Results in Engineering 21 (2024) 101925. https://doi.org/10.1016/J.RINENG.2024.101925.
[17] L.J. Habeeb, A. Mohammed, Natural Convection Heat Transfer in Horizontal Annuli with Inner Elliptic and Circular Cylinder, n.d.
[18] JR Senapati, S.K. Dash, S. Roy, Numerical investigation of natural convection heat transfer from vertical cylinder with annular fins, International Journal of Thermal Sciences 111 (2017) 146–159. https://doi.org/10.1016/j.ijthermalsci.2016.08.019.
[19] H. Laidoudi, M. Helmaoui, Enhancement of natural convection heat transfer in concentric annular space using inclined elliptical cylinder, Journal of Naval Architecture and Marine Engineering 17 (2020) 89–99. https://doi.org/10.3329/jname.v17i2.44991.
[20] H. Laidoudi, Buoyancy-driven flow in annular space from Two circular cylinders in tandem arrangement, Metallurgical and Materials Engineering 26 (2020) 87–102. https://doi.org/10.30544/481.
[21] R. Hosseini, A. Rezania, M. Alipour, L.A. Rosendahl, Natural convection heat transfer from a long heated vertical cylinder to an adjacent air gap of concentric and eccentric conditions, Heat and Mass Transfer/Waerme- Und Stoffuebertragung 48 (2012) 55–60. https://doi.org/10.1007/s00231-011-0840-6.
[22] A. Nouri-Borujerdi, M.E. Nakhchi, Heat transfer enhancement in annular flow with outer grooved cylinder and rotating inner cylinder: Review and experiments, Appl Therm Eng 120 (2017) 257–268. https://doi.org/10.1016/j.applthermaleng.2017.03.095.
[23] X. Yuan, F. Tavakkoli, K. Vafai, Analysis of natural convection in horizontal concentric annuli of varying inner shape, Numeri Heat Transf A Appl 68 (2015) 1155–1174. https://doi.org/10.1080/10407782.2015.1032016.
[24] M. Miansari, M.A. Valipour, H. Arasteh, D. Toghraie, Energy and exergy analysis and optimization of helically grooved shell and tube heat exchangers by using Taguchi experimental design, J Therm Anal Calorim 139 (2020) 3151–3164. https://doi.org/10.1007/s10973-019-08653-3.
[25] T. Saha, T. Islam, S. Yeasmin, N. Parveen, Thermal influence of heated fin on MHD natural convection flow of nano-fluids inside a wavy square cavity, International Journal of Thermofluids 18 (2023) 100338. https://doi.org/10.1016/J.IJFT.2023.100338.
[26] A. Jawichian, S. Siedel, L. Davoust, Dielectrophoretic influence on free convection in a differentially heated cavity, Int J Heat Mass Transf 200 (2023) 123560. https://doi.org/10.1016/J.IJHEATMASSTRANSFER.2022.123560.
[27] A. Karami, F. Veysi, F. Aliee, A novel approach based on neural network to model the free convection within a differentially heated cavity partitioned by interior curved slats, International Journal of Thermal Sciences 189 (2023) 108281. https://doi.org/10.1016/J.IJTHERMALSCI.2023.108281.
[28] L. Jaafer, Natural Convection Heat Transfer in Horizontal Annuli with Inner Elliptic and Circular Cylinder, (n.d.). https://www.academia.edu/4312410/Natural_Convection_Heat_Transfer_in_Horizontal_Annuli_with_Inner_Elliptic_and_Circular_Cylinder (accessed September 2, 2024).
[29] A.S.A. Mohamed, M.S. Ahmed, A.G. Shahdy, Theoretical and experimental study of a seawater desalination system based on humidification-dehumidification technique, Renew Energy 152 (2020) 823–834.
https://doi.org/10.1016/J.RENENE.2020.01.116.
[30] E.I. Eid, Experimental study of free convection in an elliptical annular enclosure in blunt and slender orientations, Heat and Mass Transfer/Waerme- Und Stoffuebertragung 47 (2011) 81–91. https://doi.org/10.1007/s00231-010-0678-3.
[31] M. Cianfrini, M. Corcione, A. Quintino, Natural convection heat transfer of nano-fluids in annular spaces between horizontal concentric cylinders, in: Appl Therm Eng, 2011: pp. 4055–4063. https://doi.org/10.1016/j.applthermaleng.2011.08.010.
[32] T. Tayebi, A.J. Chamkha, Natural convection enhancement in an eccentric horizontal cylindrical annulus using hybrid nano-fluids, Numeri Heat Transf A Appl 71 (2017) 1159–1173. https://doi.org/10.1080/10407782.2017.1337990.